FAILURE MODES OF SILICON NITRIDE UNDER UNIAXIAL COMPRESSION

Stefano Guicciardi[†], Cesare Melandri[†], Davide Bigoni[‡]

[†]*IRTEC-CNR, Via Granarolo 64, Faenza, Italy*

[‡]*DISTART, Università di Bologna, Italy*

ABSTRACT

Failure modes of silicon nitride cylinders have been investigated under uniaxial compression at 1200 °C in air. Samples with different aspect ratios (h/d) have been tested: 5/2, 4/2, 2/2, and 1/2 (mm/mm). In all cases, the stress/strain curves evidence an initial linear portion followed by a peak and a slight softening. Most of the tests were interrupted at about 3-4 % of load drop after the peak, and the samples observed with optical and electronic microscope. Two samples catastrophically broke in correspondence of the test stop and further observations were precluded. In all the other cases, failure patterns were observed and involved modes which show intriguing symmetries. Particularly, surface exfoliation seems to play a central role in limiting the load-bearing capacity of the sample. The reason of such an exfoliation may be interpreted in different ways. A possibility is a surface buckling mechanism. However, in addition to this surface mode, traces of localized patterns of deformations which initiated and propagated macro-cracks can be found in some samples.

SOMMARIO

Con test di compressione a 1200 °C in aria, si sono studiati i modi di rottura di cilindri di nitruro di silicio in cui è stato variato il rapporto altezza/diametro: 5/2, 4/2, 2/2 e 1/2 (mm/mm). In tutti i casi, le curve nominali sforzo-deformazione sono caratterizzate da una parte iniziale lineare seguita da un picco e quindi un leggero "softening". Per l'analisi del danneggiamento, la maggior parte dei test è stata

interrotta dopo che il carico era sceso del 3-4 % rispetto al picco massimo e i campioni osservati al microscopio ottico ed elettronico. Nella maggior parte dei casi, la rottura avviene in modi che mostrano interessanti simmetrie. In particolare, l'esfoliazione superficiale, che può essere interpretata come un fenomeno d'instabilità superficiale, sembra giocare un ruolo dominante. In aggiunta a questo modo superficiale di rottura, in alcuni campioni sono piuttosto evidenti tracce di deformazione localizzata, da cui nucleano e propagano macro-fessure.

1. Introduction

Advanced ceramics are known to be good candidate materials for high temperature structural applications [1-5]. Unfortunately, the large use of ceramic components is limited by intrinsic limits, like the low fracture toughness, and by a poor knowledge of the mechanical behaviour under the particular conditions in which the material will operate. Being brittle materials, advanced ceramics are mainly tested in tension, as this is considered the most harmful stress condition. Anyway, to obtain fully dense components, sometimes sintering aids are needed for specific ceramics. Usually, these sintering aids remain as intergranular vitreous phase in the final microstructure of the material. Being less refractory than the ceramic itself, at high temperature, this phase becomes viscous promoting viscous flow and grain sliding when a stress is applied [6-9]. Moreover, under stress, due the high hydrostatic pressure which sets up at the triple grain boundary junction, the intergranular glassy phase is the place where cavitation occurs mostly, even in compression [10,11]. At high temperature, when the above-mentioned relaxing mechanisms come into play, both tensile and the compressive strength of the material drop. The ratio of the tensile vs. compressive strength, which at room temperature is about 1/10 [12], could be lower when the temperature is increased, depending on which failure mechanism prevails.

A few works on short-term tensile tests appeared in the literature on advanced ceramics at high temperature [13-15], while little or nothing can be found about short-term compressive tests. This study represents an initial contribution in this almost unexplored field.

2. Experimental

The selected material was prepared by mechanically mixing an α-Si_3N_4 powder (S-Stark LC 12 SX, H. C. Stark, New York, NY) with 8 wt% Y_2O_3 and 3 wt% Al_2O_3 as sintering aids. The mixture was uniaxially hot-pressed in a graphite crucible under a pressure of 30 MPa at 1810 °C. X-ray diffractometry of the as-sintered material revealed that the main phases were β-Si_3N_4 with $\approx$ 10% residual α-Si_3N_4. Some relevant microstructural and mechanical properties are summarised in Tab. 1 (measured at room temperature unless otherwise indicated). Further information can be found in [16].

From the pellet (45 mm in diameter and 15 mm height), cylinders with a diameter of 2 mm were obtained by machining with their axis parallel to the hot-pressing direction. Samples with different heights were prepared: 1 mm, 2 mm, 4 mm and 5 mm, respectively. The tests were conducted in air at 1200 °C using an Instron machine mod.6025 (Instron Ltd., High Wycombe, U.K.). To avoid excessive friction at the interface, two larger Si_3N_4 cylinders (6 mm in diameter and 3 mm in height) machined from the same billet of the samples were inserted between the sample and the alumina pushrods. All the tests were

conducted with a nominal strain rate of $5 \bullet 10^{-5}$ s^{-1}. The strain rate was calculated from the specimen height and the crosshead displacement rate. The heating rate was 10 °C/min and, before loading, the sample was allowed to soak for 18 min to insure thermal equilibrium. Most of the tests were stopped after a load drop of about 3-4 % of the peak load. The load was removed before the cooling down. Two out of nine samples broke just after the test stop. To observe the full evolution of the damage evolution, one thick sample, 1 mm height, was deformed up to 0.12. The sample failure patterns were observed by optical (Leitz DMRME, Leica, Wetzlar, Germany) and scanning electron microscope (Cambridge Instruments, Cambridge, U.K.).

3. Results and discussion

The peak load shows a slight tendency to lower when the height of the sample is increased, Fig. 1. This slenderness effect may be expected and has been also well documented for concrete [17]. Including all the values reported in Fig. 1, the peak load averages 4509 N with a standard deviation of 303 N.

A simple deconvolution may be applied to the load-displacement curves in order to

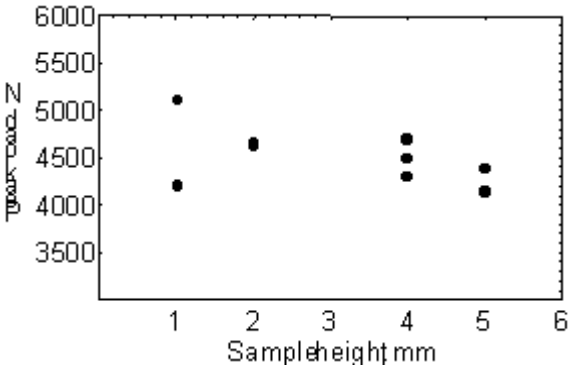

Figure 1

Compression peak loads vs. sample height for Si_3N_4 cylinders tested at 1200 °C in air.

evaluate the effective strain of the sample. The system compliance can be estimated according to the following relationship:

$$C_T = \frac{L_o}{E \cdot S} + C_S \quad (1)$$

where C_T is the total compliance, L_O the initial height of the sample, E the Young modulus, S the cross section of the sample and C_S the system compliance. Using at least three samples with different heights, it is possible to evaluate, by a linear regression analysis, the Young modulus of the material and the system compliance. Subtracting the system compliance from the measured total compliance, the true load-displacement curve of the sample (and whence the nominal stress-deformation) is obtained. The stress-strain curves calculated in this way are plotted in Fig. 2. The regression analysis gives a Young modulus value of about 105 GPa.

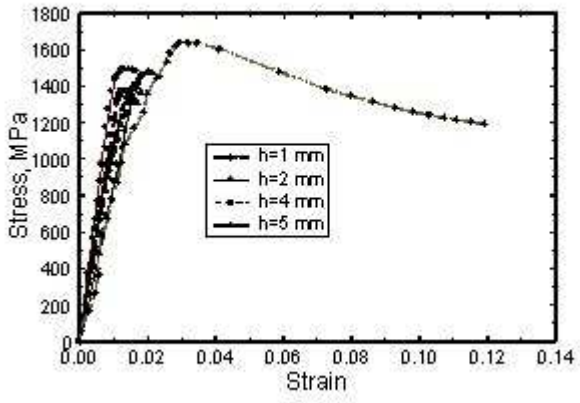

Figure 2
Compression stress-strain curves for Si_3N_4 cylinders tested at 1200 °C in air. h is the sample height.

The general shape of the stress-strain curve does not indicate any significative difference among samples with different height (this is also consistent with results presented in [17] for concrete, where the strong difference in the stress/strain curves is relative to the post-peak behavior).

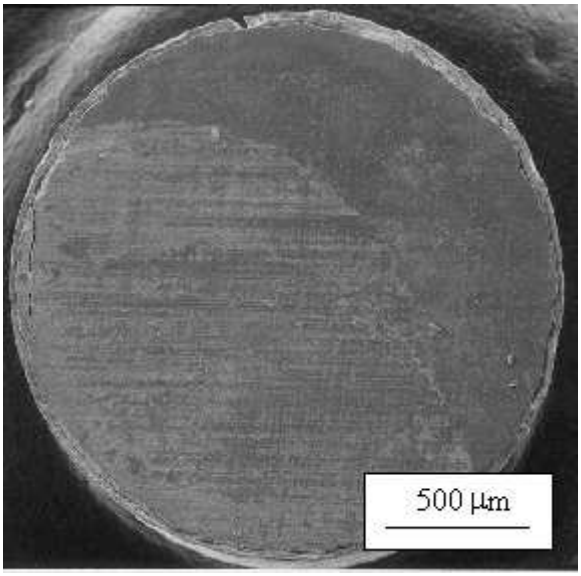

Figure 3
SEM micrograph of a sample 2 mm height after test. Top view.

SEM photographs of the samples are reported in Figs. 3-6, for different aspect ratios. Figs. 3 and 4 refer to aspect ratios 2/2 and 1/2, respectively. In both cases a surface exfoliation is evident. The exfoliation layer was quantified to be about 30÷ 35 µm, Fig. 3. Internal cracks can also be observed, Fig. 4. Surface exfoliation is also very clear from Fig. 5 (aspect ratio 4/2). However, this sample was longitudinally sectioned and cracks almost parallel to the loading direction were observed. These may be interpreted as a localized axial-splitting failure mode. The thick sample (aspect ratio 1/2) relative to Figs. 6 a,b shows once more the surface exfoliation failure mode. Interestingly, this exfoliation is in this case a progressive mechanism: at least four exfoliated layers can be detected in Fig. 6b (particular of Fig. 6a), with almost equal thickness of about 70 µm.

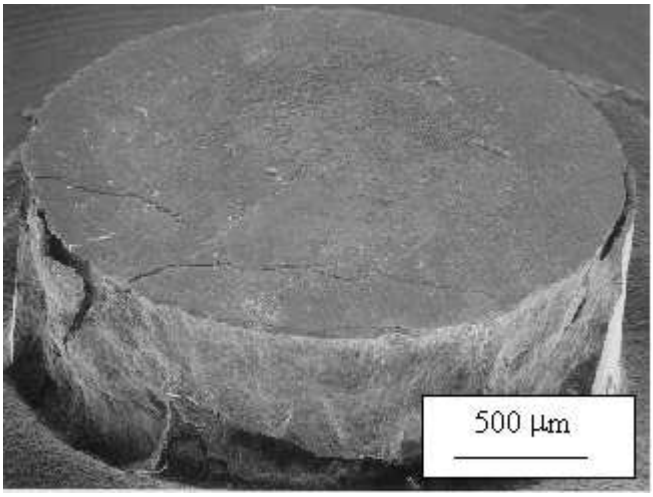

Figure 4
SEM micrograph of a sample 1 mm height after test.

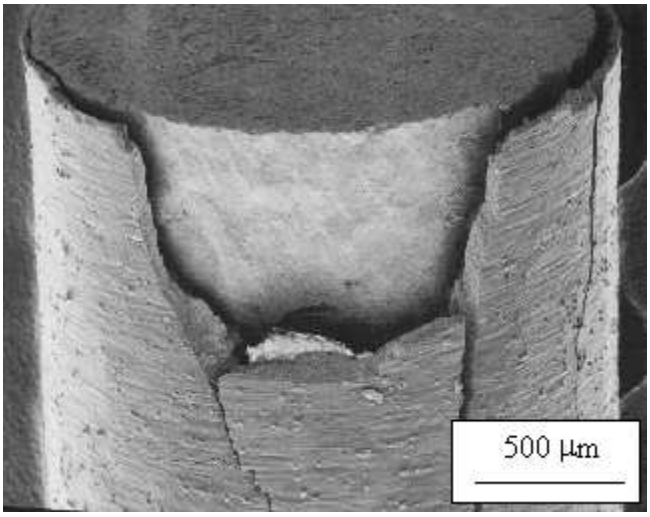

Figure 5
SEM micrograph of a sample 4 mm height after test.

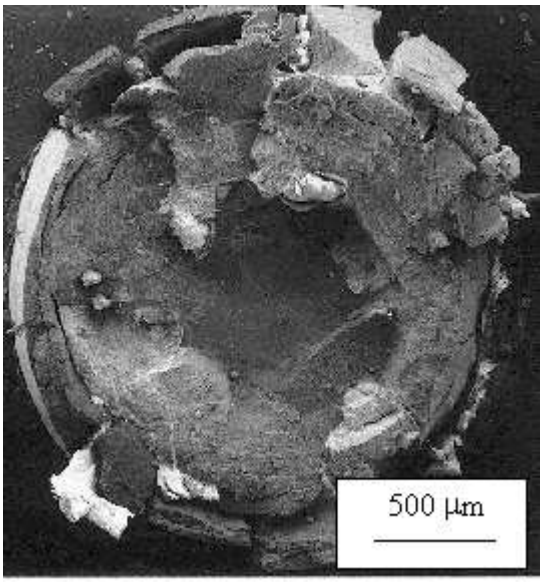

Figure 6a
SEM micrograph of a sample 1 mm height deformed up to 0.12. Top view.

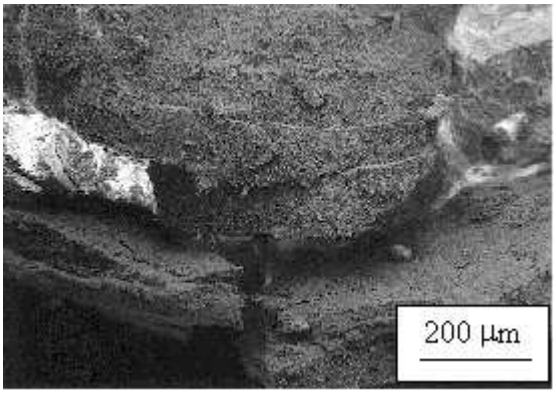

Figure 6b
Detail of micrograph 6a. Note the successive esfoliations formed during the test.

Summarizing, axially-symmetric surface exfoliation is the dominant failure mechanism. This is a well-known mechanism in rock mechanics [18] and also found in axial compression of concrete [17]. This effect can be interpreted from a number of perspectives. It can be related to the effect of friction at the specimen/cushion contact, but in our case the test set up was specifically arranged to minimize this effect. Alternatively, it may be considered the analogous for a brittle material of the surface effects observable in metal specimens [19]. From this point of view, it may be interpreted as a bifurcation phenomenon [18]: the homogeneous deformation pattern corresponding to the cylindrical shape may cease to be unique and bifurcate to an inhomogeneous pattern with surface undulations, which decay rapidly away from free surface. The problem of bifurcation of a cylindrical specimen subject to uniaxial compression was analyzed in [20] for rock-like materials. An analysis of these results reveals that the surface mode corresponds usually to bifurcation loads higher than those corresponding to barrelling or beam-like buckling modes. Therefore, the explanation of the experimental results needs to resort to some peculiar physical mechanism.

In rock mechanics, the presence of cracks parallel to the free surface is often invoked for bifurcation to occur [18]. For the analyzed material, such type of cracks are unlikely even if

not they cannot be *a priori* excluded. On the other hand, due to the fabrication process, a thin layer of material subject to residual stress may exist close to the free surface due to machining. This layer, often detected in ceramic materials [21], may give rise to a surface bifurcation mode occurring before other modes [22]. Another explanation of the observed failure patterns may come from the fact that the failure modes share similarities with the modes relative to the triaxial compression of sand specimens [23]. In these specimens, failure occurs due to localization of deformation organized in a conical geometry. Strain localization may be analyzed in terms of material instability [24]. For the material under consideration, there is not enough experimental evidence to employ a definite constitutive framework. Anyway, a rough modelling may correspond to the Drucker-Prager model [24]. For this model strain localization was thoroughly analyzed. In our case, to interpret strain localization, a localized band must be found (almost) parallel to the loading direction. For the material under consideration, the ratio tensile/compressive uniaxial yield stress may be estimated to be around 1/7. This value lies beyond the range of parameters analyzed in [24]. However, simple calculations show that a band parallel to the loading direction is predicted during softening and, for any value of plastic dilatancy, sufficiently close to the value corresponding to associativity.

4. Conclusions

Experimental results have been presented, relative to uniaxial compression at 1200 °C in air of silicon nitride cylinders. Results pertain to different diameter/height ratios. This parameter did not change the overall features of the stress-strain curve (which in the present case were interrupted just after peek) and of the failure modes. For all investigated diameter/height ratios, failure was initiated by surface exfoliation followed by the formation and growth of macrocracks. We propose three possible interpretations. These are: 1) effects related to specimen/cushion friction, which should have been minimized due to experimental set up; 2) effects related to a surface buckling as induced by machining residual stress; 3) effects related to strain localization in a cylindrical geometry.

From the performed experiments, it cannot be directly concluded whether one of the above mechanisms prevails or if there is a co-operation leading to failure.

Acknowledgements

D.B. and S.G. acknowledge financial support of M.U.R.S.T. 60%.

5. References

1. D. C. Larsen, J. W. Adams, L. R. Johnson, A. P. S. Teotia, *Ceramic Materials for Advanced Heat Engines*, Noyes Publications, Park Ridge, U.S.A., 1985.
2. N. Ichinose, *Introduction to Fine Ceramics*, John Wiley & Sons Ltd, Cichester, U.K., 1987.
3. R. W. Davidge, M. H. Van de Vorde, *Design with Structural Ceramics*, Elsevier Science Publishers Ltd, Barking, U.K., 1990.
4. G. W. Meetham, *J. Mater. Sci.*, 26, 853 (1991).
5. R. Raj, *J. Am. Ceram. Soc.*, 76, 2147 (1993).
6. R. L. Tsai and R. Raj, *Acta Metall*., 30, 1043 (1982).
7. D. S. Wilkinson and M. M. Chadwick, *J. Phys. III*, 1, 1131 (1991).
8. K. S. Chan and R. A. Page, *J. Am. Ceram. Soc*., 76, 803 (1993).
9. W. E. Lueke, S. M. Wiederhorn, B. J. Hockey, R. E. Frause, Jr., and G. G. Long, *J. Am. Ceram. Soc*., 78, 2085 (1995).
10. F. F. Lange, B. I. Davies, and D. R. Clarke, *J. Mat. Sci.*, 15, 601 (1980).
11. J. Crampon, R. Duclos, F. Peni, S, Guicciardi, G. de Portu, *J. Am. Ceram. Soc*., 80, 85 (1997).
12. A. G. Atkins, Y.-W. Mai, *Elastic and Plastic Fracture*, p. 175, Ellis Horwood Series in Engineering Science, Ellis Horwood Ltd, Chichester, U.K., 1988.
13. T. Ohji, Y. Yamauchi, W. Kanematsu, S. Ito, *J. Mater. Sci.*, 25, 2990 (1990).

14. C.-K. Jack Lin, M. G. Jenkins, M. K. Ferber, *J. Europ. Ceram. Soc.*, 12, 3 (1993).

15. T. Ohji, Y. Yamauchi, *J. Am. Ceram. Soc.*, 77, 678 (1994).

16. V. Biasini, S. Guicciardi, A. Bellosi, *Refractory Metals & Hard Materials*, 11, 213 (1992).

17. J.A. Hudson, E.T. Brown, C. Fairhurst, Proceedings 13th Symp on Rock Mech., E. J. Cording, Ed., University of Illinois Urbana Press, USA, 1971.

18. I. Vardoulakis, J. Sulem, *Bifurcation Analyisis in Geomechanics*, Chapman & Hall, UK, 1995.

19. D. Rittel, *Scripta Metallurgica et Materialia*, 24, 1759 (1990).

20. K. T. Chau, *Int. J. Solids Structures*, 29, 801 (1992).

21. R. Samuel, S. Chandrasekar, T. N. Farris, R. H. Licht, Evan *J. Am. Ceram. Soc.*, 72, 1960 (1989).

22. D. Bigoni, M. Ortiz, A. Needleman, *Int. J. Solids Structures*, 34, 4305 (1997).

23. J. Desues, R. Chambon, M. Mokni, F. Mazerolle, *Géotechnique*, 46, 529 (1996).

24. J. W. Rudnicki, J. R. Rice, *J. Mech. Phys. Solids*, 23, 371 (1975).

Atti del convegno

[Precedente] [Successiva]

Versione HTML realizzata da